Available online at www.sciencedirect.com
SCIENCE DIRECT
Journal of Power Sources 156 (2006) 461–465
JOURNAL OF POWER SOURCES
www.elsevier.com/locate/jpowsour

Short communication

Identification of nickel sulfides on Ni–YSZ cermet exposed to H_2 fuel containing H_2S using Raman spectroscopy

Jian Dong, Zhe Cheng, Shaowu Zha, Meilin Liu *

Center for Innovative Fuel Cell and Battery Technologies, School of Materials Science and Engineering, Georgia Institute of Technology, 771 Ferst Drive, Atlanta, GA 30332-0245, USA

Received 5 May 2005; received in revised form 16 June 2005; accepted 24 June 2005
Available online 11 August 2005

Abstract

Ni–YSZ cermet was exposed to hydrogen containing different concentrations of H_2S to identify the phases formed under various conditions using Raman spectroscopy and X-ray diffraction (XRD). For Ni–YSZ samples exposed to hydrogen containing 100 ppm H_2S at 727 °C for 5 days, thermodynamic calculations indicate that Ni–YSZ would be stable and XRD analysis was unable to detect any changes. However, the vibration modes of Ni_3S_2 were detected using Raman spectroscopy, suggesting that Raman spectroscopy could be a powerful tool for in situ study of sulfur poisoning of SOFC anodes. For Ni–YSZ cermet exposed to hydrogen containing 10% H_2S at 950 °C for 5 days, Ni was converted to nickel sulfide, and vibration modes of NiS were detected using Raman spectroscopy.

Keywords: Ni–YSZ cermet; Sulfur poisoning; Nickel; Raman spectroscopy; XRD

1. Introduction

Ni-based anodes are widely used for solid oxide fuel cells (SOFC). Under normal fuel cell operating conditions, nickel is susceptible to poisoning by hydrogen sulfide at concentrations as low as a few ppm [1,2]. While the performance loss caused by sulfur poisoning is reversible when H_2S concentration is sufficiently low, it becomes irreversible, at least partially, when the concentration of H_2S is relatively high (e.g. greater than 100 ppm). Dees et al. [3] reported that the interfacial polarisation resistance increased by 100% when a Ni-based anode was exposed to humidified H_2 containing 105 ppm H_2S at 1000 °C. It is suspected that H_2S may adsorb on the surface of metal electrodes and form metal sulfides [4]. Xia et al. [5] also assumed that the formation of a thin layer of Ni_3S_2 at some locations with the Ni–YSZ cermet might contribute to the anode deactivation. Here we report our recent results on studies of a Ni–YSZ cermet anode exposed to a H_2S containing atmosphere using Raman spectroscopy and X-ray diffraction (XRD). The objective of this study was to develop in situ characterisation techniques for probing and mapping gas slid interactions under fuel cell operation conditions in order to provide a theoretical basis for rational selection of potential anode materials for sulfur tolerance.

While some ultra high vacuum based surface characterisation methods, such as X-ray photoelectron spectroscopy and low energy electron diffraction, are known to be sensitive to surface species and have been used to study the adsorption of H_2S on Ni surface [6], they are not suitable for characterisation of gas–solid interaction under fuel cell operation conditions.

2. Experimental

YSZ powder (Tosoh) was dry-pressed and sintered in air at 1500 °C for 5 h. Then the NiO–YSZ composite (1:1 in volume) was sintered on the YSZ pellet surface at 1400 °C for 2 h. The pellets of NiO–YSZ/YSZ were exposed to pure H_2 at 800 °C for 2 h to convert NiO to Ni, resulting in Ni–YSZ cermet. Ni–YSZ (on YSZ) is about 10 mm in diameter and

* Corresponding author. Tel.: +1 404 894 6114; fax: +1 404 894 9140.
E-mail address: meilin.liu@mse.gatech.edu (M. Liu).

0378-7753/$ – see front matter © 2005 Elsevier B.V. All rights reserved.
doi:10.1016/j.jpowsour.2005.06.016

20 μm thick. The whole assembly was exposed to humidified (3 vol.% water vapor) hydrogen containing either 100 ppm H_2S at 727 °C or 10% H_2S at 950 °C for 5 days at a flow rate of 10 ml min^{-1}. Ni foil (99%, from Alfa Aesar) and Ni_3S_2 (containing small amount of Ni_7S_6, from Strem Chemicals) were used as the standard samples for Ni and Ni_3S_2.

Raman spectroscopy was performed using a Renishaw 2000 Raman Spectromicroscope (488 nm, 40 mW) whereas the XRD analysis was performed on a powder X-ray diffractometer (PW1800) using Cu Kα radiation.

3. Results and discussion

3.1. XRD and Raman spectra of samples exposed to hydrogen containing 100 ppm H_2S

Fig. 1(a) shows the XRD pattern of the sample after exposure to 100 ppm H_2S at 727 °C for 5 days. While the peaks corresponding to Ni and YSZ are observable (according to JCPDS card no.: 04-0850 and 82-1246), no peaks corresponding to nickel sulfides were observable in the XRD spectra. Fig. 1(b) shows the XRD pattern of the standard sample from Strem Chemicals. The reflections represent a mixture of Ni_3S_2 (according to JCPDS card no.: 44-1418) and Ni_7S_6 (24-1021). The strongest reflection of Ni_7S_6 located at 48.84° (as indicated by the arrow) is rather weak compared with that of Ni_3S_2, implying that the amount of the Ni_7S_6 in the sample is much less than that of Ni_3S_2.

After exposure to H_2S, the morphologies of the Ni–YSZ cermet appear to remain the same as that of before exposure. As shown in Fig. 2(a), three strong peaks at 208, 288 and 334 cm^{-1} appeared in the Raman spectrum for the

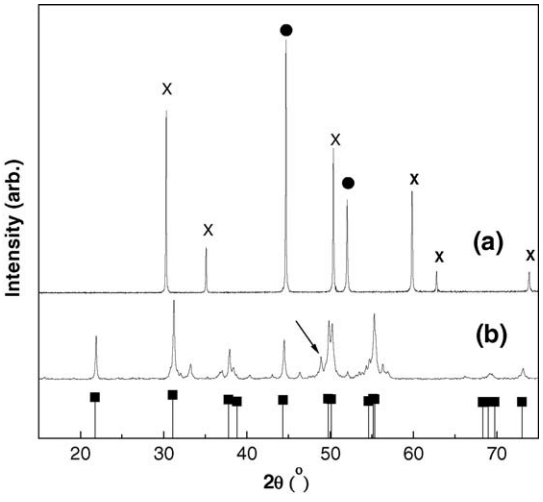

Fig. 1. XRD patterns: (a) Ni–YSZ cermet exposed to hydrogen containing 100 ppm H_2S and (b) reference Ni_3S_2 sample for comparison (containing small amount of Ni_7S_6). Reflections of Ni_3S_2 (JCPDS card no.: 44-1418) are shown in vertical lines on the bottom. The strongest peak of Ni_7S_6 in pattern of standard Ni_3S_2 sample is indicated by arrow, (×) YSZ; (●) Ni; (■) Ni_3S_2.

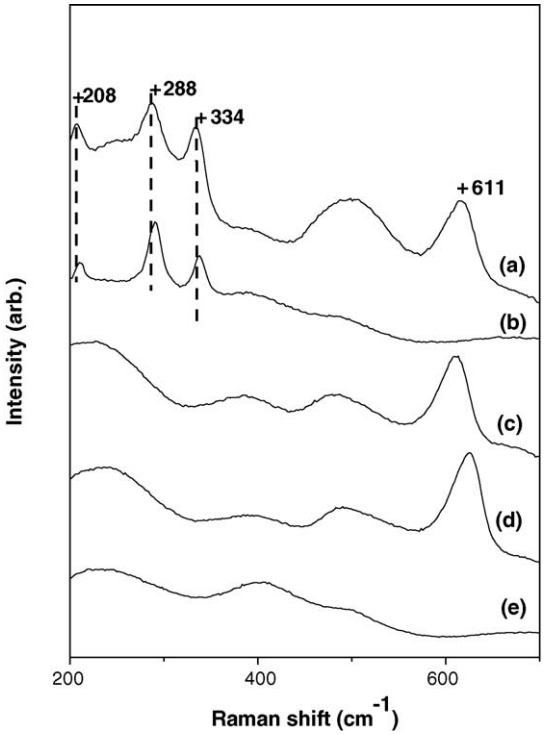

Fig. 2. Raman spectra of different samples: (a) Ni–YSZ cermet after exposure to H_2 containing 100 ppm H_2S, (b) reference Ni_3S_2 sample (containing small amount of the Ni_7S_6) for comparison, (c) Ni–YSZ cermet before exposure to H_2 containing 100 ppm H_2S, (d) YSZ pellet and (e) Ni foil.

Ni–YSZ cermet after exposure to H_2S. The Raman spectrum of Ni–YSZ cermet before exposure to H_2S is shown in Fig. 2(c). The Raman spectrum of standard Ni_3S_2 sample is shown in Fig. 2(b). Although the XRD results show a small amount of Ni_7S_6 in the reference sample, Ni_7S_6 is not Raman active [7]. As Raman is performed on standard reference sample, spectra similar to that in Fig. 2(b) can be collected in most of the particles. Therefore, the peaks of Fig. 2(b) are assigned to Ni_3S_2. This leads to the conclusion that after exposure to hydrogen containing 100 ppm H_2S, Ni_3S_2 is formed on the surface of Ni particles of Ni–YSZ cermet. In addition, the typical vibration mode of YSZ is at 611 cm^{-1} (Fig. 2(d)) and there are no vibration modes for pure Ni metal (Fig. 2(e)) in the range from 200 to 700 cm^{-1}. Since Raman spectra of YSZ before and after exposure to sulfur are the same, these new peaks are related to Ni_3S_2.

The Raman spectra suggest that, as the fresh surface of a Ni metal is exposed to a sulfur containing fuel, the active sites of Ni adsorb H_2S and further react with H_2S to form nickel sulfides, thus blocking the active sites for oxidation of fuel (such as H_2) and degrading the fuel cell performance. This seems to be consistent with Xia's hypothesis that Ni_3S_2 formed on Ni–YSZ cermet surface accounts for the anode deactivation.

While nickel sulfide was detected by a surface sensitive technique such as Raman spectroscopy, no nickel sulfide was detected by XRD. The observed strong reflections of {1 1 1} and {2 2 0} of Ni in the XRD pattern suggest that the bulk Ni

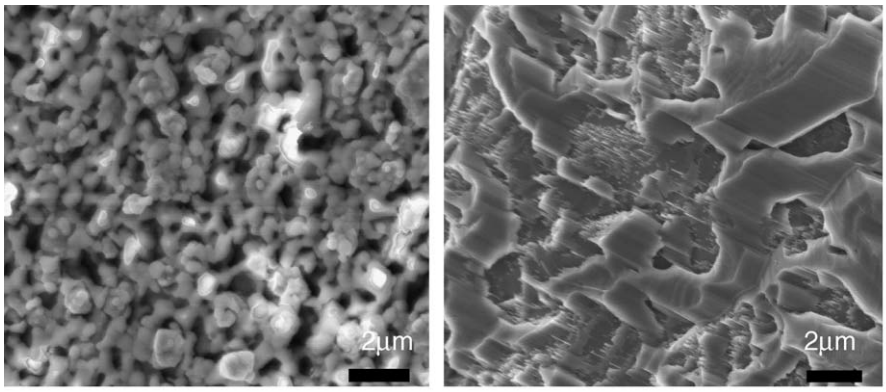

Fig. 3. SEM images of Ni–YSZ cermet exposed to H_2 containing different concentration of H_2S: (a) 100 ppm and (b) 10%.

was not affected by the exposure to H_2S of Ni. In addition, shown in Fig. 3(a) are the SEM images of the Ni–YSZ cermet after exposure to H_2S. The morphology of the Ni–YSZ cermet after exposure to H_2S appears to be the same as that exposed to pure H_2.

The thermodynamics of the Ni–S system have been well studied in previous investigations [8]. The Gibbs free energy changes for the reactions between solid Ni and H_2S to form different nickel sulfides phase are estimated from the thermochemical data in the literature [9,10]. Fig. 4 shows the Gibbs free energy change as a function of H_2S partial pressure for the formation of bulk NiS_2, $0.5Ni_3S_4$, 2NiS and Ni_3S_2 phases at 727 °C in humidified H_2. The free energy change is more negative for the formation of nickel sulfide with higher Ni:S ratio, but the formation of bulk nickel sulfides is energetically unfavorable under the condition for H_2S exposure experiment (i.e., 727 °C, 100 ppm H_2S in humidified H_2).

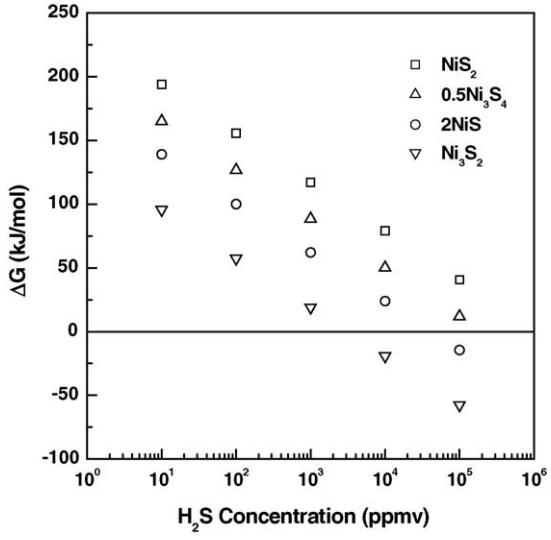

Fig. 4. Gibbs free energy change vs. H_2S concentration for the formation of different nickel sulfides at 727 °C in 97% H_2/3% H_2O. The raw data are taken from references [9,10].

It is noted that the thermochemical data presented here are for the bulk phases under equilibrium conditions. If there were local, nanoscale surface roughness, the molar free energy for Ni at the "nanoscale bump" would be significantly higher than that for the smoother, bulk Ni phase. In fact, the excess free energy for spherical particles with radius r is higher than particles with infinitely flat surfaces by ΔG_r^{ex}

$$\Delta G_r^{ex} = \frac{3}{2} P_r^{ex} V_m = \frac{3\gamma V_m}{r} \quad (1)$$

in which γ is the surface energy of the material, P_r^{ex} the excess pressure ($P_r^{ex} = 2\gamma/r$) and V_m the molar volume [11]. For nickel, $\gamma = 2.45\ J\ m^{-2}$ [12], $V_m = 6.59 \times 10^{-6}\ m^3\ mol^{-1}$, the excess energy for Ni is as high as 48 kJ mol^{-1} when $r = 1$ nm. On the other hand, the melting point of Ni_3S_2 is 789 °C under standard condition (i.e. $pH_2S = 1$) and decreases below 727 °C as pH_2S decreases below $\sim 10^{-2}$ to 10^{-3} [8,9]. If the Ni_3S_2 phase on the surface spread on nickel, the excess surface energy for it would be negligible. The combined effect may make the formation of nickel sulfide on the Ni surface with nanoscale roughness energetically possible. For example, the formation of Ni_3S_2 at local region is given by

$$3Ni_{(s,local)} + 2H_2S_{(g)} = Ni_3S_{2(l)} + 2H_{2(g)} \quad (2)$$

At 727 °C in 97% H_2/3% H_2O containing 100 ppm H_2S, the reaction free energy would be negative when $r < \sim 2.5$ nm, which is not impossible considering the Ni particles are reduced from irregular shaped NiO. As soon as those rough surface sites are consumed, no further reaction would occur. Therefore, the total amount of Ni_3S_2 would be too little to be detected by XRD. Unfortunately, no experiment result is available to directly support this hypothesis at the current stage.

3.2. XRD and Raman spectra of samples exposed to hydrogen containing 10% H_2S

The nickel sulfides and the phase relations for the nickel–sulfur system are very complicated [8,13]. Typically,

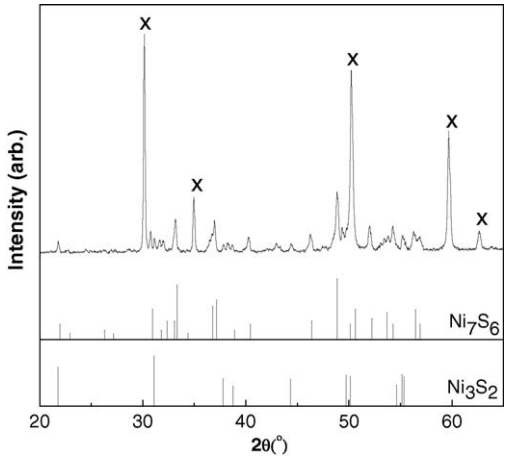

Fig. 5. XRD patterns of Ni–YSZ cermet exposed for 5 days to hydrogen containing 10% H_2S at 950 °C. For comparison, reflections of Ni_3S_2 (JCPDS card no.: 44-1418) and Ni_7S_6 (JCPDS card no.: 24-1021) are shown, respectively in vertical lines on the bottom, (×) YSZ.

Ni_3S_4 and NiS_2 dominate the sulfur-rich part of the system whereas the compounds in the Ni-rich part of the phase diagram include Ni_3S_2, Ni_6S_5, Ni_7S_6, Ni_9S_8, and NiS [14]. As some work has been done to the phase formation in the sulfidation of Inconel 738 in H_2 containing high concentration of H_2S at 500–900 °C [15], the phase formed for Ni–YSZ cermet anode is not known when it is exposed to high concentrations of H_2S.

Fig. 5 shows the XRD patterns of the Ni–YSZ cermet after exposure to 10% H_2S–H_2 at 950 °C for 5 days. Reflections of Ni metal and pure sulfur are not detected in any of the samples studied. It seems that there is no identifiable reflections of NiS. According to literature [15], however, NiS is observed in the scale of Ni alloy (Inconel 738) under similar conditions, implying that Ni particles in Ni–YSZ metal used in our study is quite different from the Ni alloys used in other studies or the amount of the NiS formed on Ni–YSZ metal is very small.

From visual observation, shining dots were found on the Ni–YSZ anode. SEM image (Fig. 4(b)) shows that the morphology of the exposed sample has completely lost the original characteristic of the Ni–YSZ cermet. These are typical images of the nickels sulfides in large size [15], suggesting that all of the nickel particles in Ni–YSZ cermet are changed to nickel sulfides as cermet exposed to high concentration H_2S. The size of these single crystals is up to 10 μm, and they are shining under the optical microscope when performing the Raman measurement. As YSZ is stable in fuel containing H_2S, and the size of the YSZ particles cannot change significantly at 700 °C, these large crystals are probably nickel sulfides. Before exposure to H_2S, the Ni particles in Ni–YSZ cermet are less than 1 or 2 μm. These large crystals may not be formed directly by reaction of Ni particles and H_2S. Small sulfides form first and then, agglomerate to large crystals when the furnace cools down because the melting point of certain types of nickel sulfides is lower than 950 °C. The

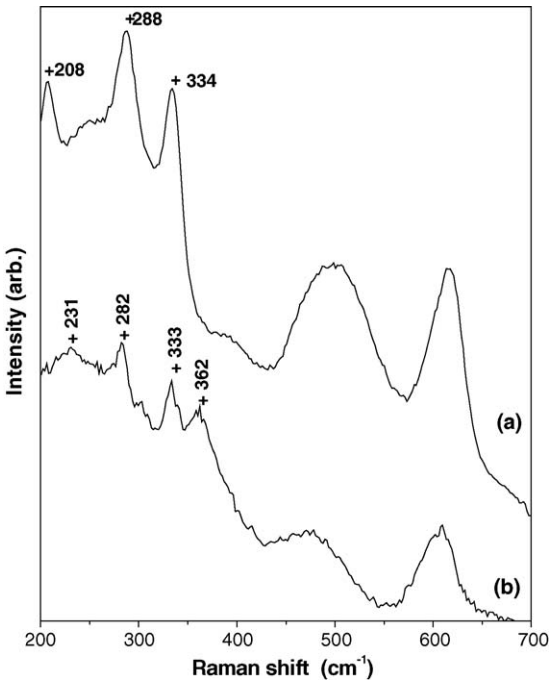

Fig. 6. Raman spectra of Ni–YSZ cermet exposed to H_2 containing different concentration of H_2S: (a) 100 ppm and (b) 10% H_2S.

XRD pattern in Fig. 5 shows that the intensity of the reflections of Ni_3S_2 in the Ni–YSZ cermet is weaker than that in Ni_7S_6. Therefore, after exposure to 10% H_2S–H_2 at 950 ° C for 5 days, nickel species in Ni–YSZ cermets are composed mainly of Ni_7S_6 with small amount of Ni_3S_2. This result is consistent with the nickel–sulfur phase diagram: Ni_7S_6 or NiS (sulfur rich phase) forms at high concentration H_2S atmosphere. While the Ni_3S_2 (sulfur deficient phase) forms at low concentration H_2S, which has already been detected by the Raman as the cermet exposed to H_2 containing 100 ppm H_2S.

Fig. 6(b) shows the Raman spectrum of Ni–YSZ cermet after exposure to hydrogen containing 10% H_2S for 5 days. Compare to cermet exposed to 100 ppm H_2S, it is noticed that one extra mode at 362 cm^{-1} is detected in addition to vibration modes at 231, 282, and 333 cm^{-1} (Fig. 6(b)). Therefore, the peaks in spectrum are assigned to NiS [16]. Compared with Ni_3S_2, NiS belongs to the sulfur rich part, and it is reasonable to believe that NiS forms at higher concentration of H_2S. Although this is different from the XRD results, it is possible that small amount of NiS co-exists on the surface of the Ni_7S_6 as the stoichiometry of Ni_7S_6 and NiS is very close.

The above analysis shows that Raman spectroscopy is very sensitive to the surface species, which is proved by detection of Ni_3S_2 on the surface of the Ni–YSZ exposed at 100 ppm concentration. Compared with the Ni–YSZ cermet exposed at 100 ppm concentration, the Raman spectrum of Ni–YSZ cermet exposed to H_2 containing 10% H_2S can be clearly differentiated, and could be reasonably assigned.

Therefore, Raman spectroscopy is rather sensitive to the phase variation of nickel sulfides. Raman spectroscopy also provides with spatial resolution on the order of 1 μm, while XRD offers no spatial resolution and has much larger penetration depth than Raman scattering. Different from XRD, low power laser beam is used as the excitation source of Raman spectromicroscope, and in situ experimental apparatus can be easily set up. As poisoning of Ni–YSZ cermet occurs on the surfaces along with electrochemical reaction at high temperatures, Raman spectroscopy has the advantage of in situ studying the poisoning mechanism over other techniques.

4. Conclusions

Raman spectroscopy has been effectively applied to detect the characteristic peaks of nickel sulfides on the surfaces of Ni particles in a Ni–YSZ cermet exposed to hydrogen containing 100 ppm H_2S at 727 °C or 10% H_2S at 950 °C for 5 days. Comparison with standard reference nickel sulfides shows that Ni_3S_2 formed on the Ni–YSZ cermet exposed to hydrogen containing 100 ppm H_2S. This gives one concrete evidence that nickel sulfide indeed forms on the Ni surface at such concentration of H_2S, which might block the active sites for oxidation of fuel (such as H_2) and degrade the fuel cell performance. It also suggests that Raman spectroscopy could be a powerful tool for in situ study of sulfur poisoning of SOFC anodes. More careful thermodynamic calculation suggests that it is reasonable for Ni_3S_2 to form on the surface of Ni particles of less than 5 nm under the conditions for H_2S exposure. As Ni–YSZ cermet exposed to hydrogen containing 10% H_2S at 950 °C for 5 days, the Ni particles are completely converted to nickel sulfides. Raman characterisation shows that NiS appears on the surface of these nickel sulfides, consistent with the prediction of Ni–S phase diagram.

Acknowledgment

This work was supported by NETL/Department of Energy SECA Core Technology Program (under Grant No. DOE-DE-FC26-04NT42219).

References

[1] A. Burke, J. Winnick, C. Xia, M. Liu, J. Electrochem. Soc. 149 (2002) D160–D166.
[2] Y. Matsuzaki, I. Yasuda, Solid State Ionics 132 (2000) 261–269.
[3] D.W. Dees, U. Balachandran, S.E. Dorris, J.J. Heiberger, C.C. McPheeters, J.J. Picciolo, SOFC-I, in: S.C. Singhal (Ed.), PV89-11, The Electrochemical Society Proceedings Series, Pennington, NJ, 1989, pp. 317–321.
[4] C.H. Bartholomew, P.K. Agrawal, J.R. Katzer, Adv. Catal. 31 (1982) 135–242.
[5] S.J. Xia, V.I. Birss, SOFC-IX, in: S.C. Singhal (Ed.), The Electrochemical Society Proceedings Series, Quebec, Canada, 2005, pp. 1275–1283.
[6] J.N. Andersen, Surf. Sci. 192 (1987) 583–596.
[7] D.W. Bishop, P.S. Thomas, A.S. Ray, Mater. Res. Bull. 35 (2000) 1123–1128.
[8] T. Rosenqvist, J. Iron Steel Inst. 176 (1956) 37–57.
[9] M.W. Chase Jr., C.A. Davies, J.R. Downey Jr., D.J. Frurip, R.A. McDonald, A.N. Syverud, JANAF Thermochemical Tables, 3rd ed., American Chemical Society, Washington, DC, 1985.
[10] M. Binnewies, E. Milke, Thermochemical Data of Elements and Compounds, Wiley-VCH, Weinheim, NY, 1999.
[11] M. Hillert, in: H.I. Aaronson (Ed.), Lectures on the Theory of Phase Transformations, 2nd ed., Minerals, Metals and Materials Society, Warrendale, PA, 1999, p. 24.
[12] A.R. Miedema, Z. Metallkd. 69 (1978) 287–292.
[13] H. Seim, H. Fjellvag, F. Grønvold, S. Stølen, J. Solid State Chem. 121 (1996) 400–407.
[14] S. Stølen, H. Fjellvag, F. Grønvold, et al., J. Chem. Thermodyn. 26 (1994) 987–1000.
[15] W. Kai, Y.T. Lin, C.C. Yu, P.C. Chen, C.H. Wu, Oxid. Met. 61 (2004) 507–527.
[16] G. Shen, D. Chen, K. Tang, C. An, Q. Yang, Y. Qian, J. Solid State Chem. 173 (2003) 227–231.